Available online at www.sciencedirect.com

SCIENCE DIRECT®

Journal of Nuclear Materials 329–333 (2004) 457–461

journal of nuclear materials

www.elsevier.com/locate/jnucmat

Mechanical properties and microstructures of high-chromium V–Cr–Ti type alloys

K. Sakai [*], M. Satou, M. Fujiwara, K. Takanashi, A. Hasegawa, K. Abe

Department of Quantum Science and Energy Engineering, Graduate School of Engineering, Tohoku University,
01 Aramaki-aza-Aoba, Aoba-ku, Sendai 980-8579, Japan

Abstract

The mechanical properties of V–Cr–Ti type alloys depended on heat treatment conditions and Cr concentrations. In this paper the correlation between mechanical properties and heat treatment conditions as a function of Cr concentrations was explored using mini-size Charpy impact tests and microstructure observations. Vanadium alloys evaluated were V–xCr–4Ti ($x = 4, 7, 10, 12, 15, 20$). Microstructure observations using transmission electron microscope (TEM) were performed to characterize the precipitates. The typical precipitates in the V–xCr–4Ti alloys were identified as Ti(C,O,N) and TiO_2. Ti(C,O,N) was observed in specimens annealed between 900 and 1000 °C and TiO_2 was between 1100 and 1200 °C. The DBTT of V–(4,7)Cr–4Ti alloys was around −190 °C, while DBTT for the other alloys were above −30 °C. It is proposed that formation of precipitates larger than 400 nm in diameter found in the alloys containing more than 10% of Cr as well as solution hardening of Cr are affected to the increase of the DBTT of the alloys.

---

1. Introduction

The V–Cr–Ti alloys are candidates for high-performance structural materials for the first-wall and blanket components of fusion reactors, because of their high temperature strength, irradiation resistance, low induced radioactivity [1–3], high thermal conductivity, and compatibility with lithium coolant [2,3]. The alloy V–4Cr–4Ti was selected as a reference material [4]. According to previous research, although higher Cr concentrations of the alloy can improve their corrosion resistance and high temperature strength, it may result in reducing their ductility and fabricability [4–6]. The mechanical properties of the alloys, even after neutron irradiation, can be improved by reducing their interstitial impurity levels as demonstrated in NIFS-heat [7] and V–Cr–Ti type alloys containing small amounts of Si, Al and Y [8,9]. In this paper, the changing in the impact property of the V–Cr–Ti alloy with various levels of Cr are described in terms of microstructure evolution, depending on heat treatment conditions.

2. Experimental procedure

The alloys V–xCr–4Ti ($x = 4, 7, 10, 12, 15, 20$) were prepared by the arc melting method at the Institute for Materials Research (IMR), Tohoku University. High-purity electrolytic Cr was used. V and Ti were used after electron beam refining. Hot forging in a vacuum was performed for the alloys V–(10,12,15,20)Cr–4Ti. The ingots were hot-rolled followed by cold-rolling to obtain the final thickness of 0.25 or 2.0 mm. Chemical compositions of the alloys are listed in Table 1. TEM-disks were punched from the 0.25-mm-thick sheet and Charpy specimens were fabricated from the 2.0-mm-thick sheet. These specimens were wrapped with Zr foils and annealed between 900 and 1300 °C for 3.6 or 7.2 ks in vacuum of less than 1×10^{-3} Pa. Charpy impact tests were carried out at temperatures from −196 to 200 °C

---

[*] Corresponding author. Tel./fax: +81-22 217 7924.
E-mail address: sakai@jupiter.qse.tohoku.ac.jp (K. Sakai).

0022-3115/$ - see front matter © 2004 Elsevier B.V. All rights reserved.
doi:10.1016/j.jnucmat.2004.04.089

Table 1
Chemical composition of vanadium alloys (wt%)

Alloy	V	Cr	Ti	C	O	N	H
V–4Cr–4Ti	bal.	4.275	4.250	0.0093	0.0235	0.0171	0.0005
V–7Cr–4Ti	bal.	7.170	3.650	0.0071	0.0213	0.0174	0.0006
V–10Cr–4Ti	bal.	10.55	4.145	0.0118	0.0276	0.0249	0.0009
V–12Cr–4Ti	bal.	12.25	4.095	0.0186	0.0304	0.0485	0.0011
V–15Cr–4Ti	bal.	14.46	3.950	0.0240	0.0273	0.0382	0.0015
V–20Cr–4Ti	bal.	20.10	4.120	0.0165	0.0233	0.0220	0.0012
Un-alloyed V	bal.	–	–	0.0037	0.0249	0.0221	0.0005

using an instrumented Charpy impact testing machine at the Oarai Branch, IMR, Tohoku University. The dimension of the miniaturized Charpy impact specimen was 1.5 mm × 1.5 mm × 20 mm with a 30° notch angle. To obtained the same mean grain size of 17 μm, each alloy was annealed at different conditions, that is V–4Cr–4Ti at 1000 °C for 3.6 ks, V–7Cr–4Ti at 1000 °C for 7.2 ks, V–(10,12)Cr–4Ti at 1100 °C for 7.2 ks, V–(15,20)Cr–4Ti at 1200 °C for 3.6 ks. Specimens of all alloys annealed at 950 °C for 3.6 ks were also tested. Vickers micro-hardness tests were carried out at 200 gf for 30 s at ambient temperature. Microstructure observations using transmission electron microscope (TEM) at 200 kV were performed. Thin films for TEM observation were prepared using a single jet-thinning apparatus. Solution of H_2SO_4–CH_3OH (1:4 by volume) at −20 °C was used with a current of 120 mA. The precipitates were identified by energy dispersive X-ray spectroscopy (EDX) and selected-area diffraction pattern (SAD) analyses.

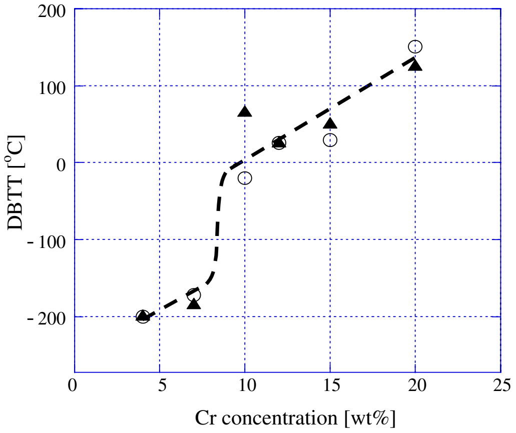

Fig. 1. DBTT of V–*x*Cr–4Ti alloys as a function of Cr concentration. Circles represent heat treatment conditions to obtain a mean grain size of 17 μm. Triangles represent heat treatment condition of 950 °C for 3.6 ks.

3. Experimental results

3.1. Mechanical properties

Fig. 1 shows ductile-brittle transition temperature (DBTT) of the V–*x*Cr–4Ti alloys as a function of Cr concentration. The DBTTs of all the specimens were higher than −30 °C except for V–4Cr–4Ti and V–7Cr–4Ti alloys. The DBTTs of V–4Cr–4Ti and V–7Cr–4Ti alloys were around −190 °C. The DBTT of the alloys increase with Cr concentration. The change was most remarkable between 7 and 10 wt% of Cr concentration. The effects of two types of heat treatment, that is the condition to obtain the same mean grain size of 17 μm or same temperature at 950 °C, on the DBTT are not significant.

Fig. 2 shows dependence of annealing temperatures on Vickers micro-hardness number for the V–*x*Cr–4Ti alloys with various Cr contents. The hardness decrease with increasing annealing temperature, thereafter the values show a minimum, and then increase with annealing temperature again. The minimum values increased with increasing Cr contents.

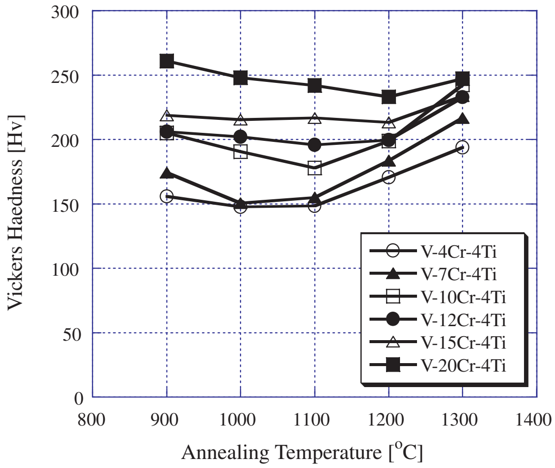

Fig. 2. Dependence on annealing temperature of Vickers hardness of V–*x*Cr–4Ti alloys.

3.2. Microstructures

Fig. 3 shows typical microstructures of the V–*x*Cr–4Ti alloys after various conditions of heat treatment. The precipitates were observed in all the specimens annealed at between 900 and 1200 °C for 3.6 ks, but not in the specimens annealed at 1300 °C. Table 2(b) and (c) shows the size and number density of the precipitates. Average diameter of the precipitates was increased, and number density was decreased with increasing annealing temperature. When Cr contents exceeded 10 wt%, large precipitates with small number densities (larger than 400 nm, $\sim 1\times10^{17}$ N_p/m^3) were observed. Table 2(a) shows identified precipitates analyzed by dark-field images and SAD patterns. EDX spectra of these precipitates indicated a Ti-rich composition. The number density and diameter of large precipitates were nearly constant for the annealing temperature between 900 and 1200 °C. According to these analyses, these precipitates are TiO and TiO_2. The TiO was observed in the specimens annealed at between 900 and 1000 °C and the TiO_2 was observed in the specimens annealed at between 1100 and 1200 °C. It is though that O positions in the TiO precipitate are partly replaced by C or N, because TiN and TiC has the same fcc NaCl-type structure with nearly same lattice parameter as TiO[10,11]. The types of precipitate did not change for the different Cr concentrations.

4. Discussions

Fig. 1 shows that the DBTT increases remarkably when Cr exceeded 10 wt%. It is believed that the increase in flow stress of the material causes the shift of the

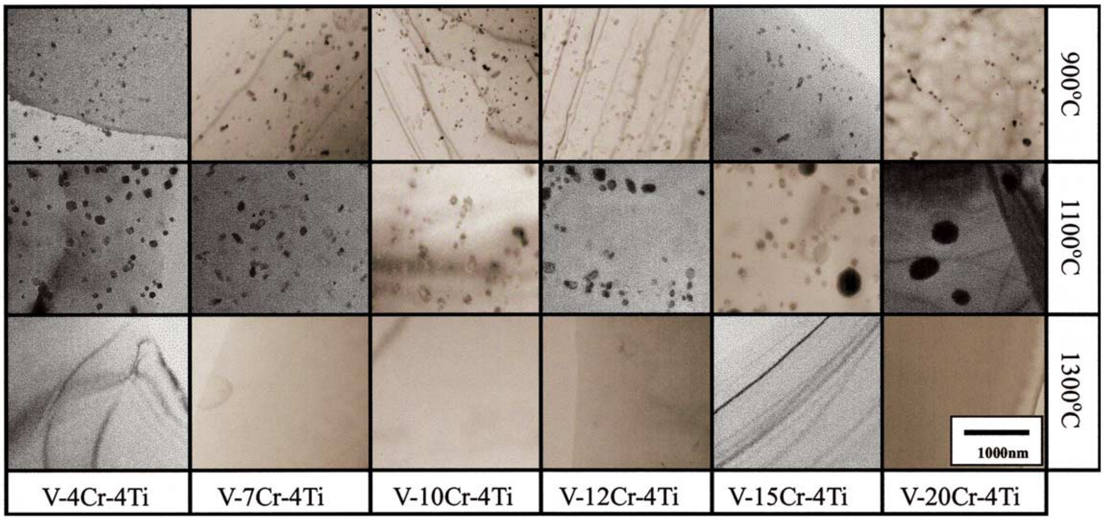

Fig. 3. Typical microstructure of V–*x*Cr–4Ti alloys heat treatment between 900 and 1300 °C for 3.6 ks.

Table 2
Summary of microstructure: (a) major precipitate, (b) average diameter [nm], (c) number density of precipitate [N_p/m^3]

	V–4Cr–4Ti	V–7Cr–4Ti	V–10Cr–4Ti	V–12Cr–4Ti	V–15Cr–4Ti	V–20Cr–4Ti
900 °C	(a) TiO	(a) TiO	(a) TiO	(a) TiO	(a) TiO	(a) TiO
3.6 ks	(b) ∼96	(b) ∼96	(b) ∼95	(b) ∼101	(b) ∼100	(b) ∼99
	(c) 2.8×10^{19}	(c) 2.4×10^{19}	(c) 3.8×10^{19}	(c) 3.9×10^{19}	(c) 2.9×10^{19}	(c) 2.2×10^{19}
1000 °C	(a) TiO	(a) TiO	(a) TiO	(a) TiO	(a) TiO	(a) TiO
3.6 ks	(b) ∼115	(b) ∼135	(b) ∼133	(b) ∼143	(b) ∼128	(b) ∼196
	(c) 3.4×10^{19}	(c) 2.1×10^{19}	(c) 2.2×10^{19}	(c) 2.4×10^{19}	(c) 2.3×10^{19}	(c) 4.1×10^{18}
1100 °C	(a) TiO_2	(a) TiO_2	(a) TiO_2	(a) TiO_2	(a) TiO_2	(a) TiO_2
3.6 ks	(b) ∼194	(b) ∼188	(b) ∼199	(b) ∼196	(b) ∼197	(b) ∼395
	(c) 1.2×10^{19}	(c) 1.1×10^{19}	(c) 1.5×10^{19}	(c) 1.4×10^{19}	(c) 1.3×10^{19}	(c) 1.1×10^{18}
1200 °C	(a) TiO_2	(a) TiO_2	(a) TiO_2	(a) TiO_2	(a) TiO_2	(a) TiO_2
3.6 ks	(b) ∼398	(b) ∼396	(b) ∼353	(b) ∼449	(b) ∼396	(b) ∼450
	(c) 1.2×10^{18}	(c) 8.1×10^{17}	(c) 2.9×10^{18}	(c) 3.5×10^{18}	(c) 3.4×10^{18}	(c) 2.5×10^{17}

DBTT. However, the dependence on Cr concentrations of the DBTT of the alloys is not as simple as the dependency of solution-hardening, that is linear correlation to Cr concentration in this range of the concentration [12]. It seems that the factors contributing to the DBTT are not only the solid-solution hardening of Cr but also the difference in precipitation behavior. The type of precipitates (Ti(C,O,N) or TiO_2) and number density did not change between 7% and 10% Cr contents. The only difference observed is the large precipitates. The relationship between the diameters (d_p) of the largest precipitates observed in the V–xCr–4Ti alloys and the DBTT is shown in Fig. 4. The DBTT is high when the largest diameter of the precipitates exceeds 400 nm. In the specimens annealed at conditions to obtain a mean gain size of 17 μm, the size of the precipitates in the V–(4,7)Cr–4Ti alloys was as small as 120 nm in diameter, while those in the V–xCr–4Ti alloys ($x = 10$, 12, 15, 20) were over 400 nm in diameter. In the specimens annealed at 950 °C for 3.6 ks, large precipitates (about 500–1000 nm) were observed in the V–xCr–4Ti alloys ($x = 10$, 12, 15, 20). The large precipitates could act as initiation points for brittle cleavage fracture, consequently, fracture stress decrease. The high DBTT can be affected by decrease in fracture stress. The large precipitates observed in the V–xCr–4Ti alloys ($x = 10$, 12, 15, 20) were probably formed during the fabrication process. In the fabrication process, melting time for mixing of the alloying elements of the alloys containing higher Cr was longer than that of the alloys with lower Cr contents. Hot forging was performed for the V–(10,12,15,20)Cr–4Ti alloys. Therefore possible contamination from the atmosphere resulted in higher gaseous impurity level of the alloys. It may be necessary to reduce the level of gaseous impurities such as C, O and N to prevent such large precipitate formation. Selection of heat treatment condition may also be possible to avoid such precipitation. These large precipitates disappeared in the specimens annealed above 1300 °C. Other types of precipitates (TiO_2) were also observed in the specimen annealed at 1100 °C for 3.6 ks. The contribution of these precipitates to strengthening is as small as 30–40 MPa from the estimation using the following equation, assuming the precipitates are Orowan type obstacles:

$$\sigma = M\alpha\mu b\sqrt{\sum_{\min}^{\max}(Nd_p)},$$

where M is the Taylor factor (= 3.1), α is the barrier strength (= 0.5), μ is the shear modules (= 46.7 GPa), b is the burgers vector (= 0.262 nm), N is the number density, d_p is the mean diameter. N (number density) and d_p (diameter) were determined from microstructure observation. These precipitates are also the evidence that Ti has a scavenging effect for oxygen atoms in the alloys. In the specimens annealed at 1300 °C, the precipitates disappeared. Titanium and oxygen were in solution so that the hardness numbers of the specimens were increased due to the solution-hardening, as shown in Fig. 2.

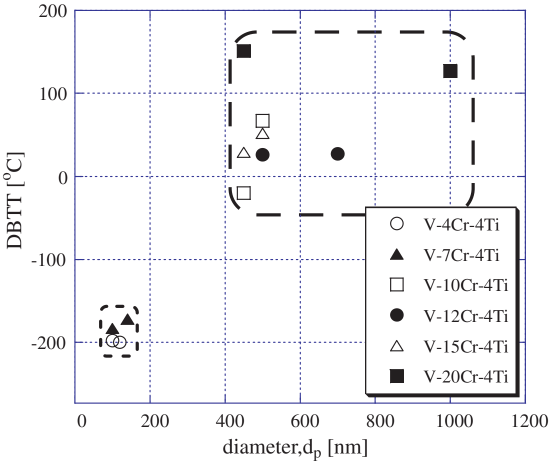

Fig. 4. Relationship between the diameter (d_p) of the largest precipitates and the DBTT of V–xCr–4Ti alloys. Two plots for each alloy represent the different condition of heat treatments as described in the manuscript.

Charpy impact properties of the alloys can be affected by increase in flow stress and decrease in fracture stress. The V–Cr–Ti type alloys containing high Cr show high flow stress due to solution-hardening by Cr, and have possible contamination of gaseous impurities such as oxygen result in formation of the large precipitates (larger than 400 nm). The large precipitates can be act as initiation point of crack. Consequently, it seems that the high DBTT of V–xCr–4Ti alloys ($x = 10$, 12, 15, 20) were caused by high flow stress caused by solid solution of Cr and initiation of crack formation caused by the large precipitates.

5. Summary

Microstructures and mechanical properties of the V–xCr–4Ti alloys ($x = 4$, 7, 10, 12, 15, 20) were examined.

1. The DBTT of V–4Cr–4Ti and V–7Cr–4Ti alloys were around −190 °C, while the alloys containing more than 10 wt% Cr were above −30 °C. It is possible to increase Cr concentrations as high as 7 wt% for V–xCr–4Ti alloy without degrading impact properties by means of controlling the formation of precipitates.
2. The DBTT increased with Cr concentrations, corresponding to the increase of flow stress due to solution-hardening by Cr. It is proposed that formation of precipitates larger than 400 nm in diameter also contributed to the shift of the DBTT of the alloys by acting as crack initiation points.

3. The typical precipitates in the V–*x*Cr–4Ti alloys were identified as Ti(C,O,N) and TiO_2. Ti(C,O,N) was observed in the specimens annealed between 900 and 1000 °C and TiO_2 in the specimens annealed between 1100 and 1200 °C.

Acknowledgements

The authors gratefully acknowledge the contributions of Dr T. Shishido, Institute for Materials Research, Tohoku University, to the preparation of the samples. This work was partly supported by the JUPITER-II program (Japan–USA Program of Irradiation/Integration Test for Fusion Research) and a Grant-in-Aid for Scientific Research from the Ministry of Education, Culture, Sports, Science and Technology, Japan.

References

[1] R.J. Kurtz, K. Abe, V.M. Chernov, V.A. Kazakov, G.E. Lucas, H. Matsui, T. Muroga, G.R. Odette, D.L. Smith, S.J. Zinkle, J. Nucl. Mater. 283–287 (2000) 70.
[2] D.R. Diercks, B.A. Loomis, J. Nucl. Mater. 141–143 (1986) 1117.
[3] D.L. Smith, B.A. Loomis, D.R. Diercks, J. Nucl. Mater. 135 (1985) 125.
[4] B.A. Loomis, H.M. Chung, L.J. Nowicki, D.L. Smith, J. Nucl. Mater. 212–215 (1994) 799.
[5] M. Fujiwara, K. Natesan, M. Satou, A. Hasegawa, K. Abe, J. Nucl. Mater. 307–311 (2002) 601.
[6] B.A. Loomis, G. Wigginsi, J. Nucl. Mater. 122&123 (1984) 693.
[7] T. Muroga, T. Nagasaka, K. Abe, V.M. Chernov, H. Matsui, D.L. Smith, Z.-Y. Xu, S.J. Zinkle, J. Nucl. Mater. 307–311 (2002) 547.
[8] M. Satou, T. Chuto, A. Hasegawa, K. Abe, ASTM, STP-1366, 2000, p. 1197.
[9] T. Chuto, M. Satou, A. Hasegawa, K. Abe, T. Nagasaka, T. Murog, J. Nucl. Mater. 307–311 (2002) 555.
[10] H.M. Chung, L.J. Nowicki, D.L. Smith, DOE/ER-0313/11, 1991, p. 215.
[11] T. Schober, D.N. Branski, Metall. Trans. A 20A (1989) 1927.
[12] H.M. Chung, B.A. Loomis, D.L. Smith, J. Nucl. Mater. 239 (1996) 139.